Hindawi Publishing Corporation
Journal of Nanomaterials
Volume 2016, Article ID 2368630, 10 pages
http://dx.doi.org/10.1155/2016/2368630

Research Article

Silver Nanoparticles Embedded in Natural Rubber Films: Synthesis, Characterization, and Evaluation of *In Vitro* Toxicity

Caroline S. Danna,[1] Dalita G. S. M. Cavalcante,[1] Andressa S. Gomes,[1] Leandra E. Kerche-Silva,[1,2] Eidi Yoshihara,[3] Igor O. Osorio-Román,[4] Leandra O. Salmazo,[5] Miguel A. Rodríguez-Pérez,[5] Ricardo F. Aroca,[4] and Aldo E. Job[1]

[1]*Departamento de Física, FCT-UNESP, 19060-900 Presidente Prudente, SP, Brazil*
[2]*Agência Paulista de Tecnologia de Agronegócios, Polo Regional Alta Sorocabana, 19160-000 Presidente Prudente, SP, Brazil*
[3]*Universidade do Oeste Paulista, 19050-920 Presidente Prudente, SP, Brazil*
[4]*Department of Chemistry and Biochemistry, University of Windsor, Windsor, ON, Canada N9B 3P4*
[5]*Cellular Materials Laboratory (CellMat), Condensed Matter Physics Department, University of Valladolid, 47011 Valladolid, Spain*

Correspondence should be addressed to Aldo E. Job; job@fct.unesp.br

Received 20 April 2016; Accepted 16 June 2016

Academic Editor: Xuping Sun

Natural rubber (NR) films can reduce silver metal ions forming embedded metal nanoparticles, a process that could be described as green synthesis. The NR films acting as a reactor generate and incorporate silver nanoparticles (AgNPs). Organic acids and amino acids play a crucial role in the formation of AgNPs. The plasmon extinction obtained in the UV-visible spectrum shows the presence of nanoparticles in the film after dipping the NR film into a solution of silver nitrate at 80°C. Electron microscopic analysis confirms the presence of AgNPs in the NR film and characterization by atomic force microscopy shows a change in the roughness of the NR film with AgNPs. In addition, our preliminary results from *in vitro* toxicity studies (MTT and comet assays) of the NR films and NR films with silver nanoparticles (NR/Ag) show that they are not toxic to cell lineage CHO-K1 (cells from the ovary of a Chinese hamster), an important result for potential medical applications.

1. Introduction

Plasmonic [1] films fabricated with metallic nanoparticles embedded in natural or synthetic polymeric materials are extensively studied, since they have potential for applications in new technologies [2, 3] and in the medical field [4, 5].

Natural rubber is a natural polymer used in the manufacture of various materials used in health care and thin film technologies [6–8]. It is a biocompatible polymer capable of inducing the angiogenesis process [9] and is being marketed in form of cream-gel REGEDERM® to aid in the healing process of cutaneous wounds. This natural polymer can also be used to induce the formation of metal nanoparticles [10, 11]. Metallic nanoparticles, in particular silver nanoparticles, are the subject of studies regarding the interactions of these particles in biological environments, such as interaction with bacteria and fungi [12–16], interaction with human cells [17, 18], and also the implications generated when AgNPs interact with DNA [19, 20]. Correspondingly, new material combining the properties of NR and silver nanoparticles opens possible avenues for new applications. A main concern is the biocompatibility of these new materials, since they could be toxic or produce genotoxicity depending on their concentrations and dimensions. The NR film provides an

active substrate acting as reducing agent and stabilizer of the metallic nanoparticles, producing a material with encapsulated AgNPs and improved biocompatibility.

In this study we evaluate the *in vitro* biocompatibility of incorporated AgNP within a polymeric matrix. The work focuses on characterizing the NR film without and with silver nanoparticles. The appearance of plasmon absorption band in UV-visible attests to the presence of metal nanoparticles. Film characterization is carried out using FT-infrared spectra, electron microscopy images, atomic force microscopy (AFM), and elemental analysis. In addition, toxicity studies were performed through the techniques of MTT and comet assays.

2. Experimental Section

2.1. Materials. Natural Rubber Latex (NRL) was collected from different trees of *Hevea brasiliensis* tree RRIM 600 clone, at Indiana Farm (Experimental Farm), located in the Indiana city, near Presidente Prudente, São Paulo State, Brazil. The latex collected was stored in a dark vessel, with capacity of 1 liter and 20 mL of ammonia hydroxide, that is, 2% v/v, was added to prevent spontaneous coagulation. Silver nitrate salt (ACS reagent, ≥99.0%) was purchased from Sigma-Aldrich and used as received. Cell line used in this study was CHO-K1 (cells from the ovary of a Chinese hamster). Cells were cultured in 10 mL of DMEM/F10 supplemented by 10% fetal bovine serum in 25 cm^2 flasks and kept in an incubator with CO_2 at 37°C.

2.2. Natural Rubber Film (NR) Preparation. NR films were prepared by depositing 10 mL of NRL in a Petri dish measuring 95 mm in diameter and put in an oven for thermal treatment (annealing for 10 hours at 65°C), to complete the NRL polymerization. The films obtained have an average thickness of around 0.5 mm.

2.3. Synthesis of NR/Ag Film. The formation of silver nanoparticles was induced by direct reaction between NR film and silver nitrate solution. The natural rubber films were submerged into $AgNO_3$ solution, with a concentration of 3.0×10^{-5} M. Throughout the procedure, the silver nitrate solution containing the NR films was kept in a sand bath at a temperature of 80°C. The NR films were withdrawn from silver nitrate solution at different reduction times: 30 min (NR/Ag30), 60 min (NR/Ag60), 90 min (NR/Ag90), and 120 min (NR/Ag120). The results are presented in Figure 1.

2.4. Preparation of Liquid Extracts. To obtain the liquid extracts, equal surface areas of NR, NR/Ag30, NR/Ag60, NR/Ag90, and NR/Ag120 films were placed in glass Petri dishes with straight bottom 9.5 cm in diameter. To each plate 10 mL of distilled water was added. The plate was sealed with PVC film and carried to the oven heated at 37°C and maintained there for 24 hours. After this time the liquid was removed from the plate and transferred to a clean container and filtered and the pH was set to 7.4. The extracts were used to carry out the MTT and comet assays. A portion of this solution was set aside for quantification of silver content.

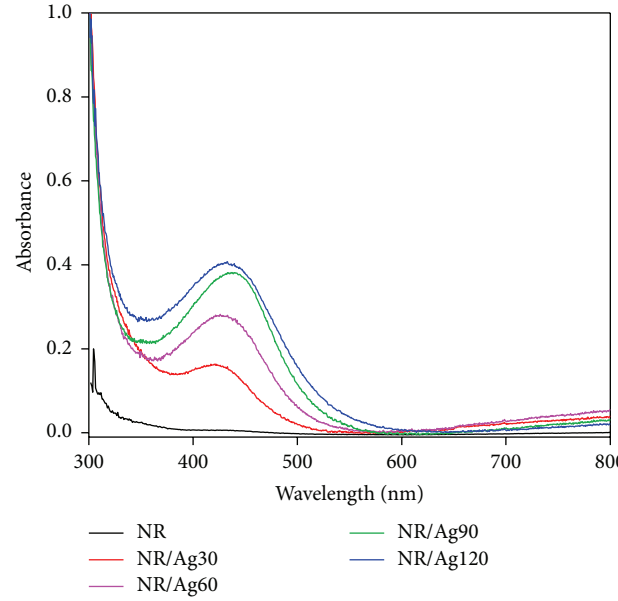

Figure 1: UV-Vis spectra of natural rubber (NR) film and NR/Ag films with different reduction times.

2.5. Exposure Protocol. For the MTT assay, the cells were seeded on a transparent 24-well plate at a density of 1.0×10^5 cells per well and taken to CO_2 incubator at 37°C for stabilization during 48 h; then the cells were put in contact with the different liquid extracts (NR, NR/Ag30, NR/Ag60, NR/Ag90, and NR/Ag120) and with distilled water for negative control (CTR). The ratio is 1 : 1 (culture media : liquid extracts or distilled water) and the cells were incubated for 24 h. For the alkaline version of the comet assay, cells were seeded at a density of 5.0×10^5 cells in transparent 12-well plate. Cells were treated for 24 hours with distilled water (CTR) or with different liquid extracts in 1 : 1 ratio.

2.6. Cellular Toxicity Evaluation

2.6.1. MTT Assay. The cytotoxic potential of extracts was assessed using the MTT reduction method [21]. Following a period of exposure (24 h), culture medium was removed, MTT solution of 0.3 mg/mL was added and cells were incubated for 4 hours. The culture medium was removed and added DMSO in order to precipitate formazan crystals. The corresponding absorbance reading was performed in a microplate reader at a wavelength of 492 nm to assess the number of viable cells in each well. The absorbance of the control was considered to represent 100% cell viability (CV). The CV of the rest of the samples was determined using the following formula:

$$\text{CVE} = \left[\frac{(\text{AE} - \text{AB})}{(\text{ACTR} - \text{AB})}\right] \times 100, \quad (1)$$

where CVE is cell viability of cells exposed to the extract; AE is absorbance of cells exposed to the extract; ACTR is absorbance of negative control cells; AB is absorbance of blank (well containing culture medium only).

2.6.2. Comet Assay. The levels of DNA damage in cells exposed to both extracts were evaluated by comet assay. Following exposure to the extracts, the adherent cells were trypsinized and were used for the preparation of the slides for the comet assay, according to the protocol described by Singh et al. [22], with a few modifications. The samples were mixed with low-melting-point agarose (0.5%), placed into glass slides, and covered with coverslips and the slides were placed in a lysis solution for a period of one hour. After the lysis step, all slides were transferred to an electrophoresis tank containing freshly prepared cold alkaline buffer. The electrophoresis was performed at 25 V and 300 mA during 20 minutes. After neutralization and fixation steps, the slides were then stained with diamidino-2-phenylindole (DAPI) (1 mg/mL *DAPI* H_2O) solution and visualized by fluorescence microscopy with 400x of magnification. One hundred nucleoids were counted per slide, and the DNA damage was visually classified into four categories according to the migration of DNA fragments, in accordance with the method described by Kobayashi et al. [23, 24]. The results were compared by parametric analysis of variance (ANOVA) using the Student-Newman-Keuls method or the nonparametric Kruskal-Wallis test, in accordance with the distribution of the data (normality and homogeneity of variance). P values < 0.05 were considered significant and the results were expressed as means ± SD (standard deviation).

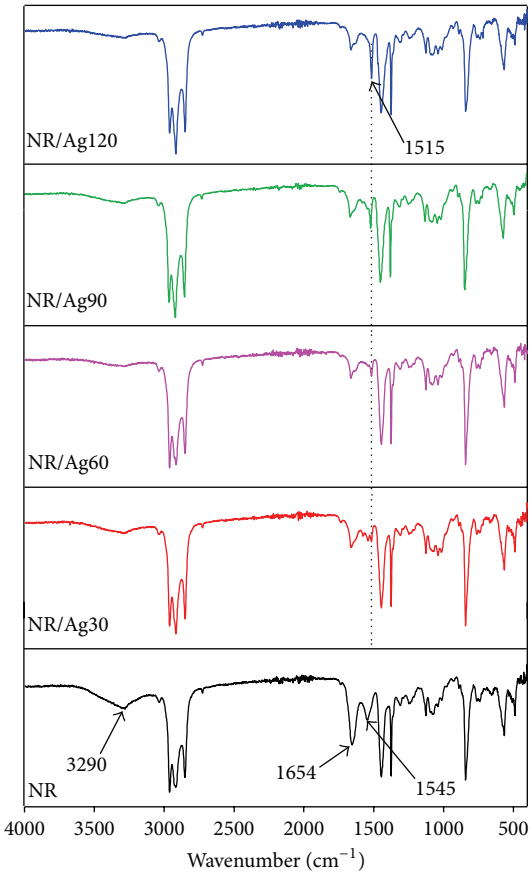

Figure 2: FT-IR spectra of natural rubber (NR) film and NR film with AgNPs at different reduction times.

2.7. Characterization Techniques

2.7.1. Characterization of NR/Ag Films. The extinction data were recorded using SHIMADZU UV-visible spectrophotometer, model UV-1800, with a scan range from 300 nm to 800 nm. The FT-IR/ATR spectral data were obtained using Bruker alpha-ATR FT-IR spectrometer, the scan range from 400 cm^{-1} to 4000 cm^{-1}. The SEM images and the elemental analysis were recorded using the Scanning Electron Microscopy (SEM) model FEI Quanta 200 FEG high microscopy resolution with EDAX Energy Dispersive Spectroscopy (EDS) and X-Ray Detector, and all the samples were coated with a thin layer of conductive carbon to improve conductivity and these measurements were performed at the Great Lakes Institute Environmental Research (GLIER), University of Windsor. Atomic force microscopy (AFM) images were recorded using a Digital Instruments NanoScope IV, operating in tapping mode with Al-coated silicon tip (model TESPA, Bruker). Images were collected with high resolution (1024 lines per scan) at a scan rate of 0.5 Hz. Digital processing of the images used the free SPM data analysis software Gwyddion 2.30. Silver content of extracts was quantified via optical emission spectrometry using inductively coupled plasma (ICP-OES); the equipment detection limit (<LoD) is 0.029 μg/mL with an error per each measurement of 0.003 μg/mL. The samples were subject to acid digestion using concentrated nitric acid followed by ICP-OES quantification using an Optima 8000 ICP-OES spectrometer Perkin Elmer.

3. Results and Discussion

Figure 1 shows the UV-Vis spectra of NR and NR/Ag films obtained in different reductions times. The NR film does not have absorption peaks, facilitating the characterization of the films with silver nanoparticles. NR/Ag films synthesized at 30 min, 60 min, 90 min, and 120 min presented typical brood plasmon absorption peaks at ~430 nm. With increase in reduction time, the intensity of the peak is proportional to the AgNPs concentration [25] and also is likely to increase size of the silver nanoparticles in the polymer matrix [26, 27]. The symmetrical shape of the plasmon indicates low dispersion of nanoparticles size formed during the reduction process [22, 23].

The vibrational spectra of neat NR films and NR/Ag films can be seen in Figure 2; the spectra were recorded at different points of the samples (5 points), and Figure 2 shows the average spectra. The NR spectrum for neat NR film agreed with the characteristic FT-IR spectrum reported in the literature [10, 28], which corresponds to that of the *cis*-isoprene structure as the other components present in the

Table 1: Important infrared absorption bands of natural rubber (NR) film and NR film with AgNPs in different times of reduction.

NR film	NR/Ag30	NR/Ag60	NR/Ag90	NR/Ag120	Assignment
3290	3287	3286	3285	3283	υ N-H amide; O-H stretch
3036	3036	3038	3034	3033	=C-H stretch
2960	2960	2961	2960	2960	υ_{as} CH form CH_3, υ_s CH from CH_3, υ_s CH_2
2915	2916	2914	2916	2916	
2852	2850	2851	2850	2849	
2724	2725	2726	2725	2725	
1654	1662	1663	1663	1662	υ C=O (amide I)
1545	1543	—	—	—	(Amide II)
—	1517	1516	1515	1515	-R_2N-H (secondary amine)
1445	1444	1446	1446	1446	Amide III, δ CH_2, δ- CH_3
1375	1374	1375	1375	1375	
1309	1308	1308	1308	1308	
1245	1247	1247	1246	1246	
1125	1125	1126	1126	1126	
1038	1040	1038	1039	1039	υ C-N/C-O
—	890	889	891	891	δ C=C-H
841	842	843	841	841	δ C=C-H
760	762	763	762	762	Amide III (N-H, C=O γ_w), skeleton of isoprene
740	742	740	739	739	

υ: stretching vibration; υ_s: symmetric stretching vibration; υ_{as}: antisymmetric stretching vibration; δ: in-plane bending vibration; δ as: antisymmetric in-plane bending vibration; γ_w: wagging vibration.

latex, such as proteins and lipids [10, 28–30]. The vibrational bands of the NR film in the 3300 cm^{-1} to 3030 cm^{-1} region are associated with the stretching modes of C-H, N-H, and O-H bonds; vibrational bands at 2960 cm^{-1} to 2850 cm^{-1} are associated with C-H bonds in lipids and the isoprene chain; vibrational bands at 1660 cm^{-1} to 1650 cm^{-1} are related to C=O stretching associated with amide I and vibrational bands at 1545 cm^{-1} are associated with amide II (protein fraction from the film); vibrational bands at 1445 cm^{-1} to 1038 cm^{-1} are associated with amide III and symmetric and asymmetric bending of the isoprene; vibrational bands at 1040 cm^{-1} to 1038 cm^{-1} are associated with the C-N and C-O stretching from 890 cm^{-1} to 840 cm^{-1}. A tentative assignment is presented in Table 1.

Notably, the intensity IR bands around 3290 cm^{-1}, 1654 cm^{-1}, and 1545 cm^{-1} decrease or disappear in NR/Ag films synthesized at 30 min, 60 min, 90 min, and 120 min. These vibrational bands are likely associated with the protein fraction of the film, playing a role in reducing the silver ions. The latter is supported by the appearance of the band at 1515 cm^{-1}, and this band is observed, with low intensity, for the NR/Ag30 film; the intensity of it increases as the reduction time lengthens. Those changes are clearly noted in the spectra shown in Figure 2, where they are indicated by dotted line. This band, according to literature, is associated with amine group (R_2-NH) [10, 28–30], and this could be a product of the synthesis, which could only come from protein denaturation or destruction of the amide bond; for this reason the bands associated with protein disappear after we put the film of latex in the solution of silver nitrate at 80°C, and the possible product of reaction between amide and Ag^+ is silver nanoparticles and amines.

Table 2: Elemental composition table for NR/Ag120 film.

Element	Wt%
CK	91.01
OK	05.09
NaK	00.23
SK	00.08
ClK	00.35
AgL	03.24

Wt%: weight percentage.

The SEM image of the surface of the NR/Ag120 film is shown in Figures 3(b) and 3(c); it is possible to observe the presence of structures that stand out of the matrix, which is the NR film; this image was chosen because we are able to see clearly the lighter dots representing the metal nanostructures in the sample (they are identified with a yellow arrow); those nanoparticles have a size between 20 nm to 60 nm. To confirm the nature of the observed particles an elemental analysis was performed, shown in Figure 3(a). The spectrum in Figure 3(a) shows the emission peak of the X-rays of silver (AgL) for the point indicated in Figure 3(b). The elemental composition values are shown in Table 2, and the percentage of silver is 3.24% mass, and this percentage refers to the point indicated by the yellow arrow in Figure 3(b). On the other hand, the size of particles observed in Figures 3(b) and 3(c) corroborates the results shown in Figure 1 (UV-Vis) where it

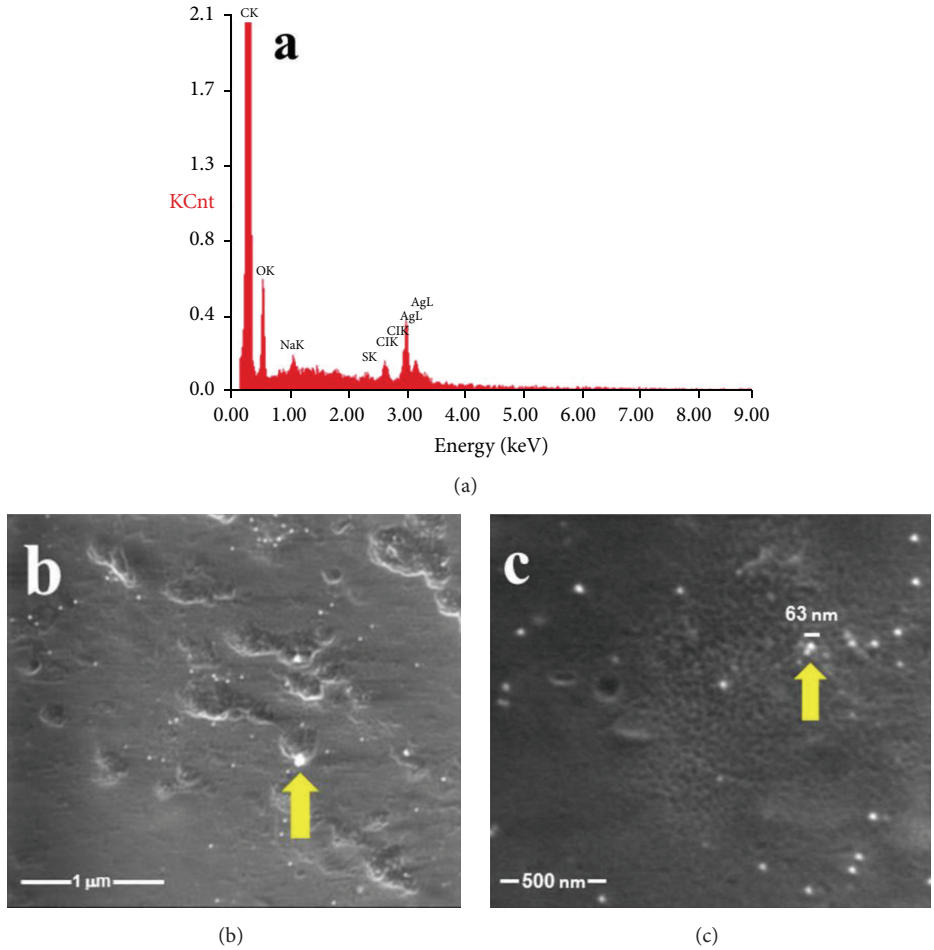

Figure 3: Elemental analysis of the NR/Ag120 film, emission peak of the X-rays (a), and Scanning Electron Microscopy (SEM) images of NR/Ag film (b and c).

is possible to observe plasmon band with maximum around 430 nm, which according to the literature [27] corresponds to silver nanoparticles that have this size.

AFM images are given in Figure 4 for neat NR film and films produced in different reduction times NR/Ag30, NR/Ag60, NR/Ag90, and NR/Ag120. Analyzing the AFM images is possible to observe film surface roughness changes. The values of root mean square average roughness (Rq) were 78.8 nm, 33.7 nm, 32.0 nm, 24.1 nm, and 20.1 nm for NR film, NR/Ag30, NR/Ag60, NR/Ag90, and NR/Ag120, respectively. These changes is directly associated with increasing the reduction time; in other words, the roughness of this surface decreases with increasing synthesis time. This fact could be associated with the growth of AgNPs at film structure; once the higher time of synthesis is related to the bigger amount of nanoparticles, then they occupy the spaces into the matrix, and the surface becomes smoother.

It is necessary to assess whether the NR/Ag films have biological characteristics compatible to be defined as a biomaterial. Two important characteristics of biomaterials are biocompatibility and biofunctionality [31]. Among the various biocompatibility tests required, *in vitro* cytotoxicity and genotoxicity tests are the first two assays conducted to begin to assess the biocompatibility of a new material [32, 33]. Among the various existing *in vitro* cytotoxicity assays, the MTT test is the most commonly used; using this methodology the cell viability is quantified by conversion of tetrazolium into formazan by mitochondria viable cells [34]. In this sense we test our films without and with silver nanoparticles with MTT assay. To support the essay, we analyzed whether extracts free any compound after 24 hours using inductively coupled plasma optical emission spectrometry (ICP-OES) (see Figure 5). The quantification results show that the total silver concentrations for NR/Ag30 and NR/Ag60 liquid extract are above the detection limit (0.029 μg/mL), and the amount is approximately 0.17 μg/mL and 0.07 μg/mL, respectively (see Figure 5). The latter means that the NR/Ag film releases silver in distilled water used to make the liquid extract. For the extracts NR, NR/Ag90, and NR/Ag120 the total silver released was not identified or was below the detection limit; that is, the films prepared with higher reduction times are not releasing silver when placed in solution. One explanation for the detection of silver in the extracts obtained from NR/Ag30 and NR/Ag60 may be

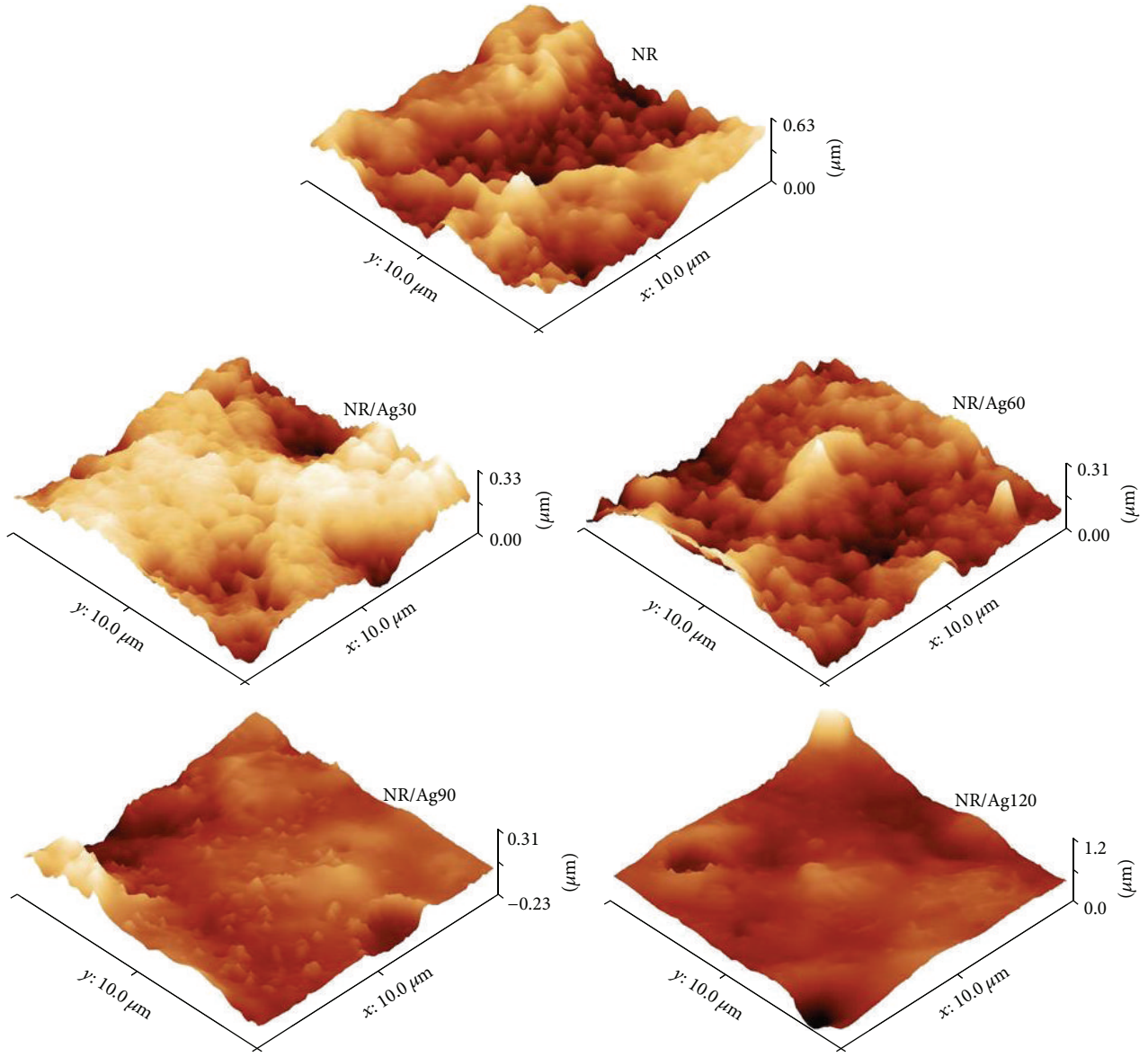

Figure 4: Atomic force microscopy (AFM) images for NR film and films in different reduction times NR/Ag30, NR/Ag60, NR/Ag90, and NR/Ag120.

related to the time of reduction of silver nanoparticles. In other words, the interaction between silver nanoparticles and natural rubber films is more effective when the high reduction times occurs. It should be emphasized that in the NR/Ag30 and NR/Ag60 extracts total silver has been identified, but the amount of silver found in the extract did not cause toxic effect for cell viability of CHO-K1 lineage.

The results of MTT assay are shown in Figure 6. The bar graph shows the results for all samples and control; in Figure 6(a) we show an image of the CHO-K1 cells exposed to liquid extract from NR film in time zero; in Figure 6(b) we show the same cell culture after 24 hours of exposition by liquid extract; it is possible to observe mild differences between the two images, because the liquid extract has low toxicity (<10%), and it can be seen that the extract made with NR film and the extracts of films with silver nanoparticles with different concentration were not cytotoxic to the cell lineage tested in comparative with negative control. When measuring the cytotoxicity of a material from its extract, it is expected to evaluate whether this material can release toxic compounds for extracting vehicle [35]. It is reasonable to assume that the low toxicity associated with silver nanoparticles released to extractor vehicle for the studied cell line could be related to the synthesis route used to obtain the nanoparticles, since the use the NR film itself as a reducing agent and stabilizer for nanoparticles does not use organic chemicals commonly used in literature. The most satisfying explanation for the low toxicity is that our material contains encapsulated AgNPs and prevents the release of silver to the liquid extract. Most toxicity studies developed with nanoparticles in solution [18,

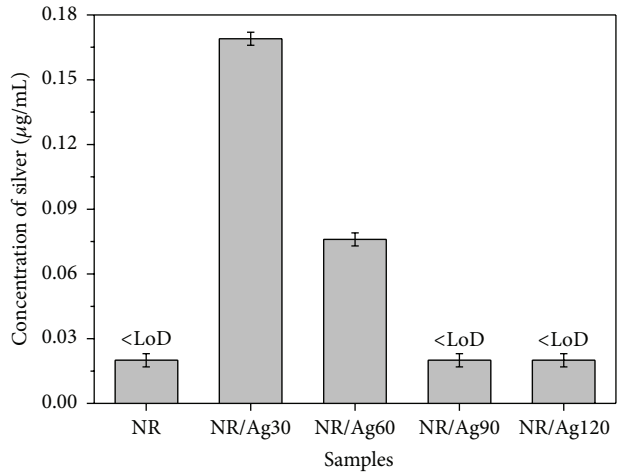

Figure 5: Concentration of silver (Ag^+) obtained through inductively coupled plasma optical emission spectrometry (ICP-OES) of the liquid extract obtained by the immersion for 24 hours in distilled water of NR and NR/Ag films obtained with different reductions times.

36–39] show that the silver concentration is directly related to cytotoxicity, and our results are in agreement with these findings, since the silver concentration released by NR/Ag films is very low.

In the cytotoxicity tests, genotoxicity tests are also important to evaluate a biomaterial. The comet assay is a widely used and very sensitive method for the evaluation of damage to DNA molecule [40]. The comet assay results are shown in Figure 7. It is found that there is no DNA damage for exposed cells to extract made from NR and the extract made from NR/Ag films compared with the negative control. For NR/Ag90 and NR/Ag120 extracts no cytotoxicity was expected, because the silver was not detected in the extracts by ICP-OES. de Souza et al. [41] conducted a study in which two cell cultures (CHO-K1 and CHO RS5) were exposed to different concentrations of AgNPs (0.025 to 5.0 μg/mL) for 24 hours and concluded that the increase of genotoxic damage is dose-dependent and the genotoxic effects are related to concentrations equal to or bigger than 1.25 μg/mL, and these results can be references to confirm the results presented in this paper, because the silver concentration in liquid extract is below toxic concentration. We could say that the key of low toxicity for our material is the fact that nanoparticles are incorporated into the film; for this reason the silver release is restricted and presents a low toxicity. In the future we must consider a prolonged period of incubation (longer than 24 hours) for film immersed in water, to reinforce the idea that films with AgNPs are not degraded and do not release toxic compounds to the cells. We must also study other cell lines to improve our biological approach. The results discussed here open the possibility for different redirection to our material. The NR/Ag30 and NR/Ag60 films can be directed to applications in the biomedical area, once those films release silver, from the matrix, and this characteristic gives them a bactericidal capacity, since the use of materials releasing silver as an antimicrobial agent is already well described in the

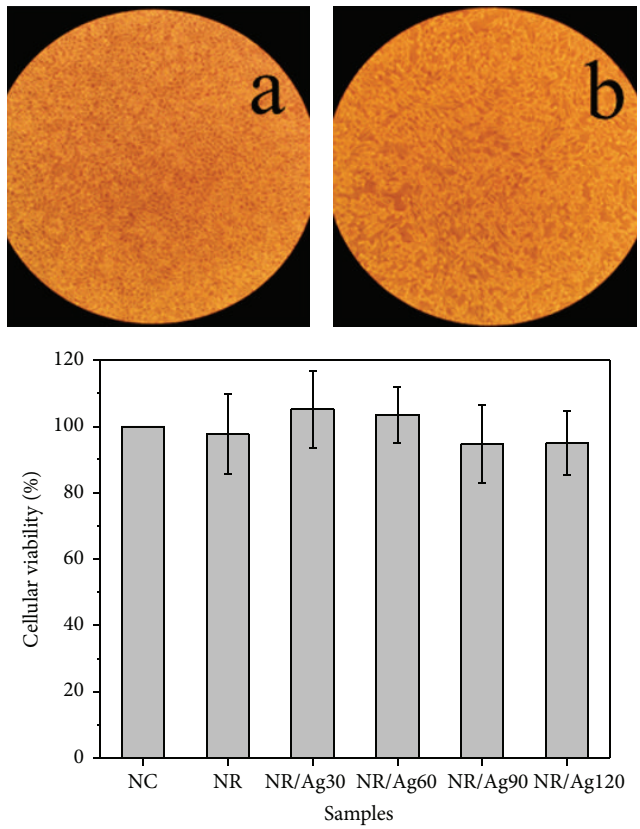

Figure 6: MTT test for liquid extract obtained by immersion for 24 hours in distilled water of NR and NR/Ag films. Image of CHO-K1 cell exposed to liquid extract of NR film at time zero (a) and image of CHO-K1 cell after 24 hours of exposure (b).

literature [42]. Already NR/Ag90 and NR/Ag120 films would be directed to technological applications, where you have the need for flexible polymer electrooptical properties [43].

4. Conclusion

The synthesis of flexible NR/Ag films with silver nanoparticles is demonstrated. Natural rubber films are used as reducing agent to form incorporated silver nanoparticles. Electron microscopy results show that homogeneity of the nanoparticles distribution on surface of the films and the size of those nanoparticles vary around from 65 nm to 85 nm. Plasmon absorption and elemental analysis confirm the presence of silver in the NR/Ag films. Preliminary cytotoxicity studies demonstrated that this new film material does not cause damage to the metabolism, nor genetic damage to the studied cell line, and these results may open the door for direct bioapplications.

Competing Interests

The authors declare that they have no competing interests.

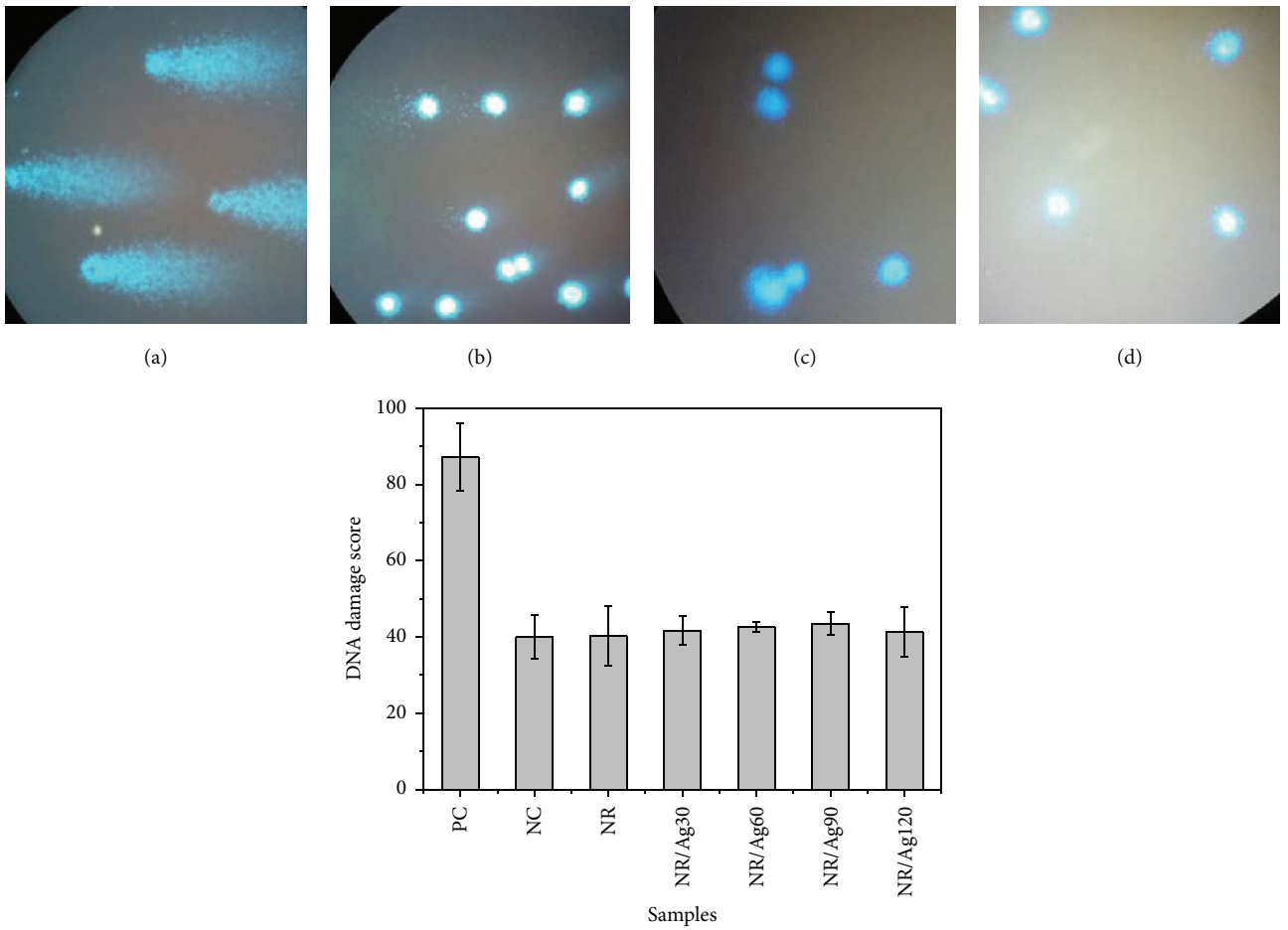

Figure 7: Comet assay for liquid extract obtained by immersion for 24 hours in distilled water of NR and NR/Ag films. On (a, b, c, and d) it is possible to observe the comet assay. Positive control (PC) (a), negative control (NC) (b), NR film (c), and NR/Ag film (d).

Acknowledgments

The authors acknowledge Fundação de Amparo a Pesquisa do Estado de São Paulo (FAPESP), the Coordenação de Aperfeiçoamento de Pessoal de Nível Superior (CAPES), the Universidade do Oeste Paulista (UNOESTE), and Agência Paulista de Tecnologia dos Agronegócios (APTA).

References

[1] S. A. Maier, *Plasmonics: Fundamentals and Applications*, Springer, New York, NY, USA, 2007.

[2] P. Shivapooja, Q. Yu, B. Orihuela et al., "Modification of silicone elastomer surfaces with zwitterionic polymers: short-term fouling resistance and triggered biofouling release," *ACS Applied Materials & Interfaces*, vol. 7, no. 46, pp. 25586–25591, 2015.

[3] H. L. Filiatrault, R. S. Carmichael, R. A. Boutette, and T. B. Carmichael, "A self-assembled, low-cost, microstructured layer for extremely stretchable gold films," *ACS Applied Materials & Interfaces*, vol. 7, no. 37, pp. 20745–20752, 2015.

[4] Q. Wei, T. Becherer, S. Angioletti-Uberti et al., "Protein interactions with polymer coatings and biomaterials," *Angewandte Chemie—International Edition*, vol. 53, no. 31, pp. 8004–8031, 2014.

[5] N. D. Stebbins, M. A. Ouimet, and K. E. Uhrich, "Antibiotic-containing polymers for localized, sustained drug delivery," *Advanced Drug Delivery Reviews*, vol. 78, pp. 77–87, 2014.

[6] C. P. Davi, L. F. M. D. Galdino, P. Borelli, O. N. Oliveira Jr., and M. Ferreira, "Natural rubber latex LbL films: characterization and growth of fibroblasts," *Journal of Applied Polymer Science*, vol. 125, no. 3, pp. 2137–2147, 2012.

[7] C. Ereno, S. A. C. Guimarães, S. Pasetto et al., "Latex use as an occlusive membrane for guided bone regeneration," *Journal of Biomedical Materials Research Part A*, vol. 95, no. 3, pp. 932–939, 2010.

[8] R. D. Herculano, C. P. Silva, C. Ereno, S. A. C. Guimaraes, A. Kinoshita, and C. F. de Oliveira Graeff, "Natural rubber latex used as drug delivery system in guided bone regeneration (GBR)," *Materials Research*, vol. 12, no. 2, pp. 253–256, 2009.

[9] M. Ferreira, R. J. Mendonça, J. Coutinho-Netto, and M. Mulato, "Angiogenic properties of natural rubber latex biomembranes and the serum fraction of *Hevea brasiliensis*," *Brazilian Journal of Physics*, vol. 39, no. 3, pp. 564–569, 2009.

[10] É. J. Guidelli, A. Kinoshita, A. P. Ramos, and O. Baffa, "Silver nanoparticles delivery system based on natural rubber latex

membranes," *Journal of Nanoparticle Research*, vol. 15, no. 4, pp. 1536–1545, 2013.

[11] F. C. Cabrera, H. Mohan, R. J. dos Santos et al., "Green synthesis of gold nanoparticles with self-sustained natural rubber membranes," *Journal of Nanomaterials*, vol. 2013, Article ID 710902, 10 pages, 2013.

[12] Y. Tian, J. Qi, W. Zhang, Q. Cai, and X. Jiang, "Facile, one-pot synthesis, and antibacterial activity of mesoporous silica nanoparticles decorated with well-dispersed silver nanoparticles," *ACS Applied Materials & Interfaces*, vol. 6, no. 15, pp. 12038–12045, 2014.

[13] M. Moritz and M. Geszke-Moritz, "The newest achievements in synthesis, immobilization and practical applications of antibacterial nanoparticles," *Chemical Engineering Journal*, vol. 228, pp. 596–613, 2013.

[14] A. G. Destaye, C.-K. Lin, and C.-K. Lee, "Glutaraldehyde vapor cross-linked nanofibrous PVA mat with in situ formed silver nanoparticles," *ACS Applied Materials & Interfaces*, vol. 5, no. 11, pp. 4745–4752, 2013.

[15] W. G. I. U. Rathnayake, H. Ismail, A. Baharin, A. G. N. D. Darsanasiri, and S. Rajapakse, "Synthesis and characterization of nano silver based natural rubber latex foam for imparting antibacterial and anti-fungal properties," *Polymer Testing*, vol. 31, no. 5, pp. 586–592, 2012.

[16] L. Sintubin, B. De Gusseme, P. Van Der Meeren, B. F. G. Pycke, W. Verstraete, and N. Boon, "The antibacterial activity of biogenic silver and its mode of action," *Applied Microbiology and Biotechnology*, vol. 91, no. 1, pp. 153–162, 2011.

[17] M. Poirier, J.-C. Simard, F. Antoine, and D. Girard, "Interaction between silver nanoparticles of 20 nm ($AgNP_{20}$) and human neutrophils: induction of apoptosis and inhibition of *de novo* protein synthesis by $AgNP_{20}$ aggregates," *Journal of Applied Toxicology*, vol. 34, no. 4, pp. 404–412, 2014.

[18] A. R. Gliga, S. Skoglund, I. Odnevall Wallinder, B. Fadeel, and H. L. Karlsson, "Size-dependent cytotoxicity of silver nanoparticles in human lung cells: the role of cellular uptake, agglomeration and Ag release," *Particle and Fibre Toxicology*, vol. 11 article 11, 2014.

[19] A. Rinna, Z. Magdolenova, A. Hudecova, M. Kruszewski, M. Refsnes, and M. Dusinska, "Effect of silver nanoparticles on mitogen-activated protein kinases activation: role of reactive oxygen species and implication in DNA damage," *Mutagenesis*, vol. 30, no. 1, pp. 59–66, 2015.

[20] S. Arora, N. Tyagi, A. Bhardwaj et al., "Silver nanoparticles protect human keratinocytes against UVB radiation-induced DNA damage and apoptosis: potential for prevention of skin carcinogenesis," *Nanomedicine: Nanotechnology, Biology, and Medicine*, vol. 11, no. 5, pp. 1265–1275, 2015.

[21] T. Mosmann, "Rapid colorimetric assay for cellular growth and survival: application to proliferation and cytotoxicity assays," *Journal of Immunological Methods*, vol. 65, no. 1-2, pp. 55–63, 1983.

[22] N. P. Singh, M. T. MCCoy, R. R. Tice, and E. L. Schneider, "A simple technique for quantitation of low levels of DNA damage in individual cells," *Experimental Cell Research*, vol. 175, no. 1, pp. 184–191, 1988.

[23] H. Kobayashi, C. Suguyama, Y. Morikawa, M. Hayashi, and T. Sofuni, "A comparison between manual microscopic analysis and computerized image analysis in the single cell gel electrophoresis assay," *Mammalian Mutagenicity Study Group Communications*, vol. 3, pp. 103–115, 1995.

[24] R. R. Tice, E. Agurell, D. Anderson et al., "Single cell gel/comet assay: guidelines for in vitro and in vivo genetic toxicology testing," *Environmental and Molecular Mutagenesis*, vol. 35, no. 3, pp. 206–221, 2000.

[25] E. J. Guidelli, A. P. Ramos, M. E. D. Zaniquelli, and O. Baffa, "Green synthesis of colloidal silver nanoparticles using natural rubber latex extracted from *Hevea brasiliensis*," *Spectrochimica Acta Part A: Molecular and Biomolecular Spectroscopy*, vol. 82, no. 1, pp. 140–145, 2011.

[26] D. R. Monteiro, L. F. Gorup, A. S. Takamiya, E. R. de Camargo, A. C. R. Filho, and D. B. Barbosa, "Silver distribution and release from an antimicrobial denture base resin containing silver colloidal nanoparticles," *Journal of Prosthodontics*, vol. 21, no. 1, pp. 7–15, 2012.

[27] Y. Qin, X. Ji, J. Jing, H. Liu, H. Wu, and W. Yang, "Size control over spherical silver nanoparticles by ascorbic acid reduction," *Colloids and Surfaces A: Physicochemical and Engineering Aspects*, vol. 372, no. 1–3, pp. 172–176, 2010.

[28] A. Barth and C. Zscherp, "What vibrations tell us about proteins," *Quarterly Reviews of Biophysics*, vol. 35, no. 4, pp. 369–430, 2002.

[29] J. Kong and S. Yu, "Fourier transform infrared spectroscopic analysis of protein secondary structures," *Acta Biochimica et Biophysica Sinica*, vol. 39, no. 8, pp. 549–559, 2007.

[30] L. K. Tamm and S. A. Tatulian, "Infrared spectroscopy of proteins and peptides in lipid bilayers," *Quarterly Reviews of Biophysics*, vol. 30, no. 4, pp. 365–429, 1997.

[31] J. Malekani, B. Schmutz, Y. Gu, M. Schuetz, and P. Yarlagadda, "Biomaterials in orthopedic bone plates: a review," in *Proceedings of the 2nd Annual International Conference on Materials Science, Metal & Manufacturing*, pp. 71–77, Global Science and Technology Forum, Bali, Indonesia, 2011.

[32] H.-C. Yang, B.-S. Lim, and Y.-K. Lee, "In vitro assessment of biocompatibility of biomaterials by using fluorescent yeast biosensor," *Current Applied Physics*, vol. 5, no. 5, pp. 444–448, 2005.

[33] C. T. Hanks, J. C. Wataha, and Z. Sun, "In vitro models of biocompatibility: a review," *Dental Materials*, vol. 12, no. 3, pp. 186–193, 1996.

[34] J. Van Meerloo, G. J. L. Kaspers, and J. Cloos, "Cell sensitivity assays: the MTT assay," *Methods in Molecular Biology*, vol. 731, pp. 237–245, 2011.

[35] H. S. Baek, J. Y. Yoo, D. K. Rah et al., "Evaluation of the extraction method for the cytotoxicity testing of latex gloves," *Yonsei Medical Journal*, vol. 46, no. 4, pp. 579–583, 2005.

[36] S. I. Kaba and E. M. Egorova, "In vitro studies of the toxic effects of silver nanoparticles on HeLa and U937 cells," *Nanotechnology, Science and Applications*, vol. 8, pp. 19–29, 2015.

[37] T. Zhang, L. Wang, Q. Chen, and C. Chen, "Cytotoxic potential of silver nanoparticles," *Yonsei Medical Journal*, vol. 55, no. 2, pp. 283–291, 2014.

[38] I. V. Vrček, I. Zuntar, R. Petlevski et al., "Comparison of *in vitro* toxicity of silver ions and silver nanoparticles on human hepatoma cells," *Environmental Toxicology*, vol. 31, no. 6, pp. 679–692, 2016.

[39] K. Kawata, M. Osawa, and S. Okabe, "In vitro toxicity of silver nanoparticles at noncytotoxic doses to HepG2 human hepatoma cells," *Environmental Science and Technology*, vol. 43, no. 15, pp. 6046–6051, 2009.

[40] S. Vandghanooni and M. Eskandani, "Comet assay: a method to evaluate genotoxicity of nano-drug delivery system," *BioImpacts*, vol. 1, no. 2, pp. 87–97, 2011.

[41] T. A. J. de Souza, L. P. Franchi, and C. S. Takahashi, "Cytotoxicity and genotoxicity of silver nanoparticles of different sizes in CHO-K1 and CHO-XRS5 cell lines," *Mutation research/Genetic Toxicology and Environmental Mutagenesis*, vol. 795, pp. 70–83, 2016.

[42] B. Le Ouay and F. Stellacci, "Antibacterial activity of silver nanoparticles: a surface science insight," *Nano Today*, vol. 10, no. 3, pp. 339–354, 2015.

[43] M. S. Miller, J. C. O'Kane, A. Niec, R. S. Carmichael, and T. B. Carmichael, "Silver nanowire/optical adhesive coatings as transparent electrodes for flexible electronics," *ACS Applied Materials & Interfaces*, vol. 5, no. 20, pp. 10165–10172, 2013.